

## Supplementary Information

### **Simultaneous realization of bulk and interface regulation based on 2,4-Diamino-6,7-diisopropylpteridine phosphate for efficient and stable inverted perovskite solar cells**

Zhen He,<sup>a, b</sup> Jian Xiong,\*<sup>a</sup> Yongsong Zhang,<sup>a</sup> Fu Liu,<sup>a</sup> Naihe Liu,<sup>a</sup> Junqian Dai,<sup>a</sup> Yongchao Liang,<sup>c</sup> Zheling Zhang,<sup>a</sup> Dongjie Wang,<sup>a</sup> Yu Huang,<sup>a</sup> Qiaogan Liao,<sup>a</sup> Jiang Wang\*<sup>a, b</sup> and Jian Zhang\*<sup>a</sup>

<sup>a</sup> Engineering Research Center of Electronic Information Materials and Devices (Ministry of Education), Guangxi Key Laboratory of Information Materials School of Materials Science and Engineering, Guilin University of Electronic and Technology, Guilin 541004, P. R. China.

<sup>b</sup> School of Mechanical and Electrical Engineering, Guilin University of Electronic Technology, Guilin 541004, P. R. China

<sup>c</sup> School of Big Data and Information Engineering, Guizhou University, Guiyang 550025, P. R. China.

\*Corresponding author: xiongjiankyxx@163.com; waj124@guet.edu.cn;  
jianzhang@guet.edu.cn

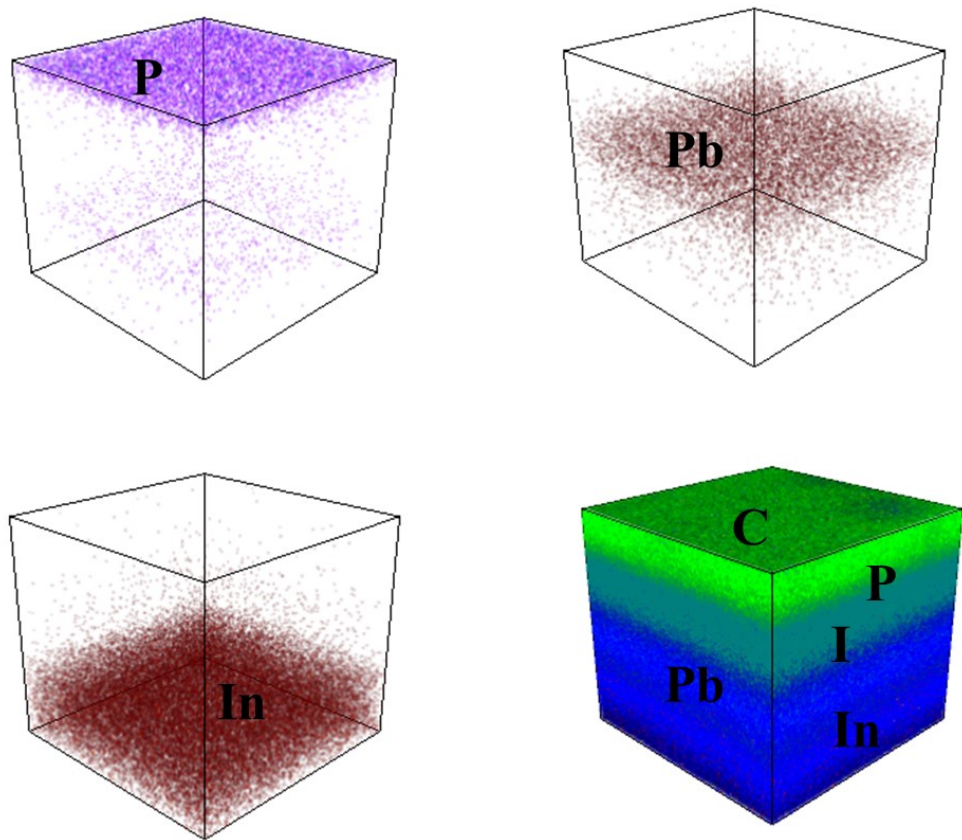


**Fig. S1.** The TOF-SIMS for depth profiling in ITO/PTAA/MAPbI<sub>3</sub>/PCBM/DPP/Ag device.

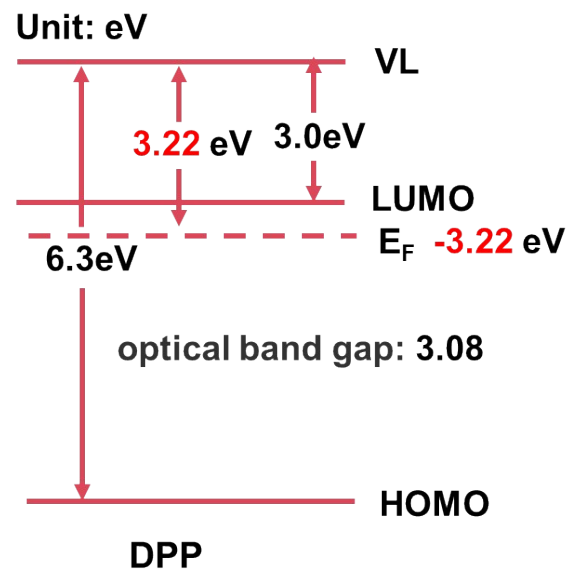


**Fig. S2.** Energy levels of DPP.

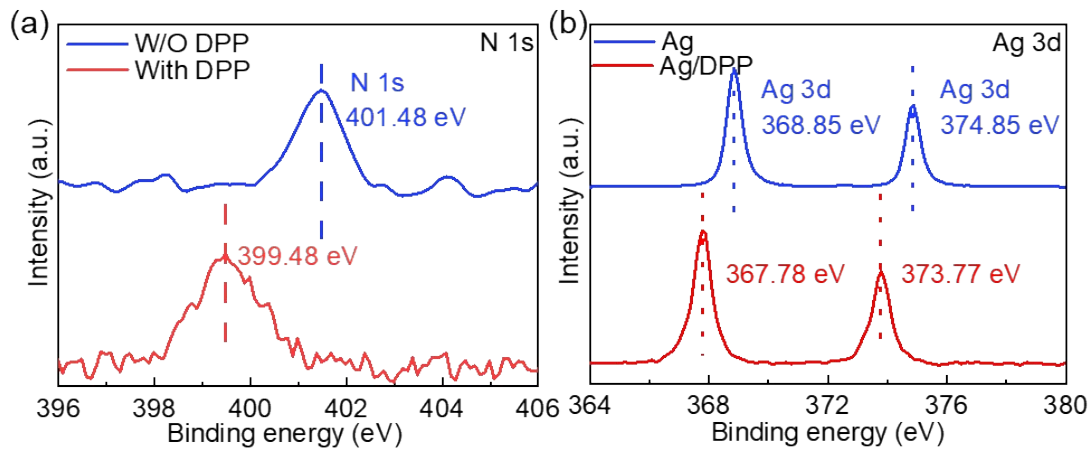


**Fig. S3.** The XPS of N 1s for ITO/PTAA/MAPbI<sub>3</sub> and ITO/PTAA/MAPbI<sub>3</sub>/DPP films. (b) The XPS of Ag 3d for Ag and DPP/Ag films.

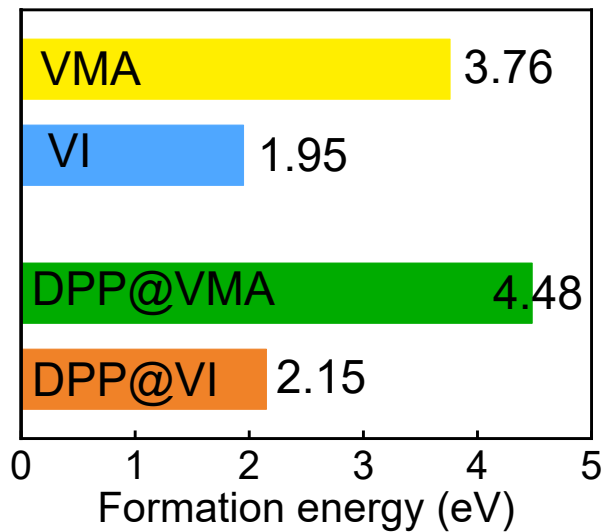


**Fig. S4.** Formation energy of MA and I vacancy defects.

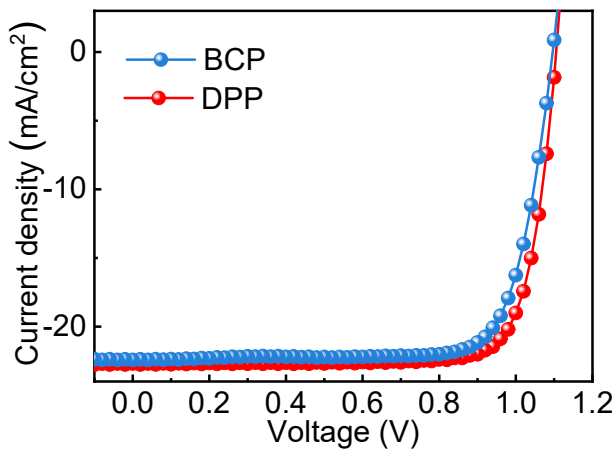


**Fig. S5.** The J-V curves of the typical BCP device and DPP device.

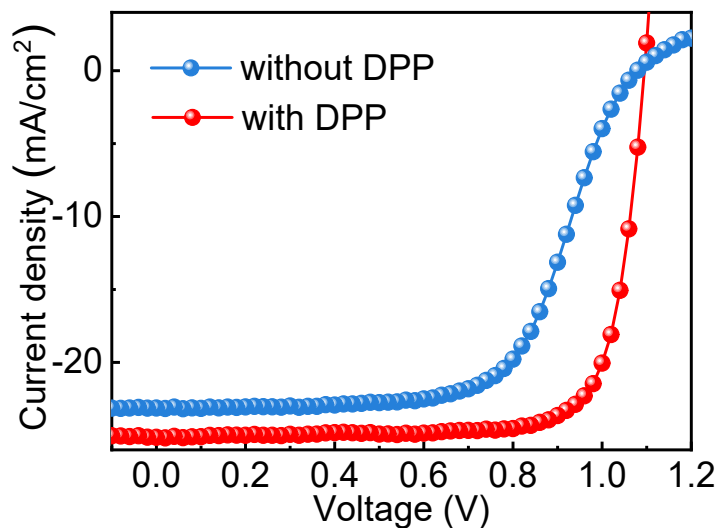


**Fig. S6** The J-V curves of the typical inverted PSCs based on  $\text{Cs}_{0.15}\text{FA}_{0.85}\text{Pb}(\text{I}_{0.95}\text{Br}_{0.05})_3$  perovskite composition with and without DPP.

**Table S1** The fitting parameters of TRPL spectra of quartz/MAPbI<sub>3</sub>, quartz/MAPbI<sub>3</sub>/PCBM and quartz/MAPbI<sub>3</sub>/PCBM/DPP films.

sample	$\tau_1$ (ns)	A <sub>1</sub> (%)	$\tau_2$ (ns)	A <sub>2</sub> (%)	T <sub>ave</sub> (ns)
MAPbI <sub>3</sub>	15.01	50.69	127.72	49.31	178.83
MAPbI <sub>3</sub> /PCBM	2.48	97.50	9.92	2.50	2.67
MAPbI <sub>3</sub> /PCBM/DPP	2.39	99.74	8.98	0.26	2.38

**Table S2** The average parameters of the BCP and DPP PSCs derived from 10 individual devices. The parameters of the best devices are shown in bracket.

Sample	V <sub>oc</sub> (V)	J <sub>sc</sub> (mA/cm <sup>2</sup> )	FF (%)	PCE (%)
BCP	1.092±0.02 ( 1.096 )	21.66±2.21 ( 22.43 )	77.76±2.54 ( 77.63 )	18.40±1.92 (19.09)
DPP	1.105±0.035 ( 1.110 )	22.21±1.47 ( 22.69 )	79.42±4.25 ( 80.46 )	19.53±0.64 (20.17)

**Table S3.** The hysteresis of the control and DPP devices from Figure 5d.

Sample	V <sub>oc</sub> (V)	J <sub>sc</sub> (mA/cm <sup>2</sup> )	FF (%)	PCE (%)
Control-F	1.070	19.60	71.35	14.94
Control-R	1.064	18.86	67.32	13.51
DPP-F	1.090	22.02	80.80	19.39
DPP-R	1.081	21.76	79.05	18.61

**Table S4** The average parameters of the inverted PSCs based on Cs<sub>0.15</sub>FA<sub>0.85</sub>Pb(I<sub>0.95</sub>Br<sub>0.05</sub>)<sub>3</sub> perovskite composition with and without DPP based on 10 individual devices. The parameters of the best devices are shown in bracket.

Sample	V <sub>oc</sub> (V)	J <sub>sc</sub> (mA/cm <sup>2</sup> )	FF (%)	PCE (%)
Without DPP	1.071±0.07 ( 1.079 )	21.75±4.03 ( 23.14 )	59.38±4.60 ( 63.81 )	13.82±3.34 (15.93)
With DPP	1.096±0.004 ( 1.095 )	24.39±0.75 ( 25.14 )	76.67±1.91 ( 78.16 )	20.50±1.01 (21.51)

**Table S5.** The EIS fitting parameters of control and DPP devices.

Sample	Rs ( $\Omega$ )	R <sub>rec</sub> ( $\Omega$ )	CPE1 (F)	R <sub>dr</sub> ( $\Omega$ )	CPE2 (F)
Control	67.33	28460	$3.66 \times 10^{-9}$	$1.03 \times 10^5$	$1.89 \times 10^{-7}$
DPP	94.85	31930	$4.33 \times 10^{-9}$	$1.08 \times 10^5$	$1.29 \times 10^{-7}$